11-4-2003

The electronic structure of metal/alkane thiol self-assembled monolayers/metal junctions for magnetoelectronics applications

Y.A. Ovchenkov
University of Nebraska - Lincoln

H. Geisler
Xavier University, New Orleans, LA

J.M. Burst
University of New Orleans, New Orleans, LA

S.N. Thornburg
University of New Orleans, New Orleans, LA

C.A. Ventrice Jr.
University of New Orleans, New Orleans, LA

See next page for additional authors

Published in *Chemical Physics Letters* 381:1-2 (November 4, 2003), pp. 7–13. doi:10.1016/j.cplett.2003.09.078 http://www.sciencedirect.com/science/journal/00092614

Submitted June 9, 2003; revised September 7, 2003; published online October 14, 2003.

The electronic structure of metal/alkane thiol self-assembled monolayers/metal junctions for magnetoelectronics applications

Y. A. Ovchenkov[a], H. Geisler[b], J. M. Burst[c], S. N. Thornburg[c], C. A. Ventrice, Jr.[c], Chunjuan Zhang[d], J. Redepenning[d], Y. Losovyj[e], Luis Rosa[a], P. A. Dowben [a,*], and B. Doudin[a]

[a] *Department of Physics and Astronomy, University of Nebraska-Lincoln, 116 Brace Laboratory, P.O. Box 880111, Lincoln, NE 68588-0111*

[b] *Department of Chemistry, Xavier University, New Orleans, LA 70125*

[c] *Department of Physics, University of New Orleans, New Orleans, LA 70148*

[d] *Department of Chemistry, University of Nebraska-Lincoln, Lincoln 68588-0304*

[e] *Center for Advanced Microstructures and Devices (CAMD), Louisiana State University, Baton Rouge, LA 70806*

Abstract: Long-chain alkane thiols use in metal to organic self-assembled monolayer to metal junctions may be limited by orientational disorder, and photoemission studies suggest that several molecular layers may be needed for the dielectric layer to be effective. Several alkane thiols were investigated in a range of junctions areas 10–10^2 μm^2. Top layer contact deposition, activated with Pd clusters resulted in a high yield of junctions that were not electrically shorted and are stable over a wide temperature range. Zero-bias anomalies, observed at low temperatures, are attributed to a Coulomb blockade associated with the Pd clusters.

1. Introduction

Metal–insulator–metal (MIM) tunnel junctions are of great interest for applications as magnetic sensors and memory devices. If both metals are ferromagnetic, the tunnel resistance of the system depends on the relative magnetic orientations of the two magnetic layers [1]. The magnitude of this effect (typically reaching 40%) depends on the properties of the insulator. The main desirable properties are the possibility to make very thin barriers (thinner than 1 nm), with atomically sharp interfaces. To date, the vast majority of tunnel magnetic junctions have been constructed using Al_2O_3 barri-

* *Corresponding author. Email:* pdowben@unl.edu *(P. A. Dowben).*

ers, but other materials have been considered as alternatives to the dielectric barrier layer.

In particular, the molecular orientation of thiols and bonding of "self-assembled" layers of alkane thiols have attracted much attention over the last two decades [2–14], and have been thought to be effective dielectric barrier layers [15, 16]. It is well documented that a variety of organic thiols can be used to construct self-assembled monolayers (SAM) on metallic surfaces [2–4]. A bonding configuration, on gold, with the molecular axis tilted 20–30° off the surface normal has be commonly identified for many alkane thiols [2, 6, 11, 12, & 17], though a planar orientation is observed for submonolayer films formed from the vapor [4, 10]. For Ag(1 1 1), a smaller tilt angle for long-chain alkane thiols, in the vicinity of 13°, has been identified [13].

We investigated the use of thiol thin films for making thin tunnel barriers. Photoemission spectroscopy measurements have been performed that give insight into the electronic properties of these films. Novel methods have been developed to make the top metallic film using electrochemical techniques. Our data show that junctions can be made without metallic shorts, but are unlikely to be of a single molecule in thickness. The results indicate that while these films may be suitable for making new spintronics devices, the barrier layer structure may be quite complex.

1.1. Photoelectron spectroscopy measurements

In order to determine the electronic structure of the thiol films, valence band photoemission was taken at the Center for Advanced Microstructure and Devices synchrotron in Baton Rouge, LA from light dispersed by a 3-m toroidal grating monochromator with electrons collected by a hemispherical analyzer. Electron collection was measured either normal to the surface ($\bar{\Gamma}$) to preserve the highest possible symmetry or with emission angles defined with respect to the surface normal. The binding energies are referenced to the substrate Fermi level. Deposition of dodecanethiol on both Au(1 1 1) and Ag(1 1 1) single crystal substrates was performed by adsorption from vapor. Vapor deposition was undertaken on substrates held at room temperature to form coverages up to one monolayer. To form multilayer coverages of thiols, the substrates were cooled below room temperature (~120 K for Ag and ~170 K for Au).

1.2. Fabrication of planar MIM junctions

Significant synthetic difficulties are encountered when trying to deposit a top metallic electrode without disrupting the organic substructure. Evaporated and sputtered metal layers are often not stable on organic thiol monolayers [18]. The high diffusion of thiols [19], as well as low structural stability of evaporated/sputtered films, usually destroys the metal/insulator/metal structure. To avoid this problem, electroless deposition was successfully used to plate ferromagnetic metal films on top of self-assembled organic tunnel barriers. Such metal films often show better structural stability than their evaporated or sputtered counterparts [20] and mechanical and thermal damage to the organic layers is avoided.

Using lithographic techniques, our metal–insulator–metal (MIM) junctions were fabricated with a planar cross geometry with junction areas ranging from 10 to 100 μm^2. Optical lithography was used to pattern lines down to a 2 μm width on silicon wafers coated with SiO_2(300 nm)/Ti(10 nm)/Au(100 nm). Ni and Co layers were then obtained by thermal deposition. An opening of a few microns was patterned using a second layer of photoresist. Depositions of alkane thiols were made in an inert atmosphere box, exposing the metallic films to a solution containing alkane thiol for 12 h. The coating solutions were comprised of ca. 0.1 M alkane thiol (ethanethiol, pentanethiol, hexanethiol or dodecanethiol) dissolved in ethyl alcohol. Thiols solution concentrations down 0.01 M and increased exposure times, up to 36 h, did not show significant changes in the tunnel junctions from the presented data. After deposition, samples were heated at 60 °C for 3 h, which diminished the fraction of junctions fabricated with electric shorts.

All alkane thiols (Aldrich) were used as purchased. Ni and Co bottom metal layers were elec-

trochemically cleaned to remove native oxides prior to "self-assembled monolayer" deposition.

Top layers of Cu and Ni were made by an electroless deposition plating process that was catalyzed by a Pd seed layer of 3–5 Å thickness, obtained by slow evaporation in a vacuum chamber. Cu films were made using a bath composition found in the literature [21]. Ni films were made using an electroless hypophosphate bath [20].

The MIM junctions were investigated in a temperature range of 1.5–300 K and under applied magnetic fields up to 10 T. Four point connections were made to perform AC and DC electrical measurements.

1.3. Evidence for dielectric character

Photoemission spectra from dodecanethiol films adsorbed on Ag(1 1 1) and Au(1 1 1) are shown in Figure 1. The saturation coverage of the thiol at room temperature is one monolayer (ML). The photoemission spectrum from the dodecanethiol submonolayer film on Ag(1 1 1) is characterized by three peaks at 10, 14, and 20 eV binding energy, as seen in Figure 1, and a peak at about 7.5 eV inferred from higher coverages and difference spectra and is accompanied by a suppression of the Ag 4d bands. Similarly, the adsorption of submonolayer coverages of dodecanethiol does lead to some suppression of the Au 5d bands with no evidence of the alkane thiols contributing any density of states in the vicinity of the Fermi level on either Ag(1 1 1) or Au(1 1 1). These results are similar to the photoemission spectra obtained for multilayer hexatriacontane Langmuir–Blodgett films on Ag(1 1 1) [14].

The formation of multilayers of thiol is achieved by deposition from the vapor on the Ag(1 1 1) or Au(1 1 1) substrate cooled to about ~120 and ~170 K, respectively. There are large shifts in the photoemission features, associated with the alkane thiol, of the multilayer film when compared to the monolayer film. The photoemission peaks are resolved at about 14, 17, 21, and 27 eV binding energy (Fig. 1). The multilayer films are insulating, with an onset of emission at ~11 eV below the Fermi level for the thicker dodecanethiol layers on Ag(1 1 1) (as seen in Fig. 1) and an onset of emission at ~5 eV below the Fermi level for the thick dodecanethiol layers on Au(1 1 1) (as seen in Fig. 1), although somewhat less in thickness than those shown on Ag(1 1 1). The large increases in binding energy are consistent with photovoltage charging as a consequence of the dielectric character of the surface and have been observed for other surface insulating layers [22]. Because of the higher deposition temperature, the thiol film on Au(1 1 1) is thinner than the film on the Ag(1 1 1), resulting in more sample charging on Ag. While this is a promising indication of the suitability of such alkane thiols as dielectric barrier layers, the insulating barrier layers should not exhibit pin-holes or provide perpendicular to the plane conduction channels.

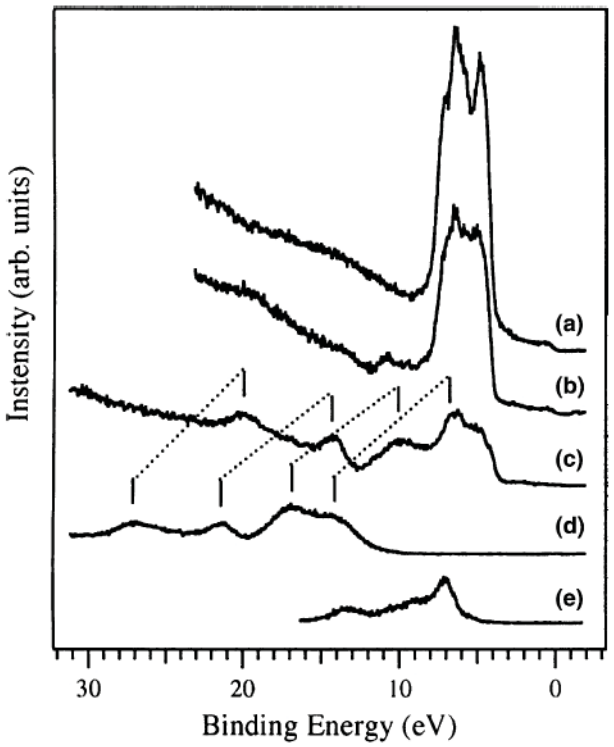

Figure 1. Normal emission, angle-resolved, photoemission spectra taken at 300 K with a photon energy of $h\nu$ = 55 eV and incident photon angle of θ = 45° for (a) clean Ag(1 1 1), (b) submonolayer of thiol on Ag(1 1 1), (c) monolayer of thiol on Ag(1 1 1), (d) multilayer of thiol on Ag(1 1 1) at 120 K, and (e) multilayer of thiol on Au(1 1 1) at 170 K taken with $h\nu$ = 84 eV and θ = 40°.

We can assign these photoemission peaks, as schematically shown in Figure 2, by comparing

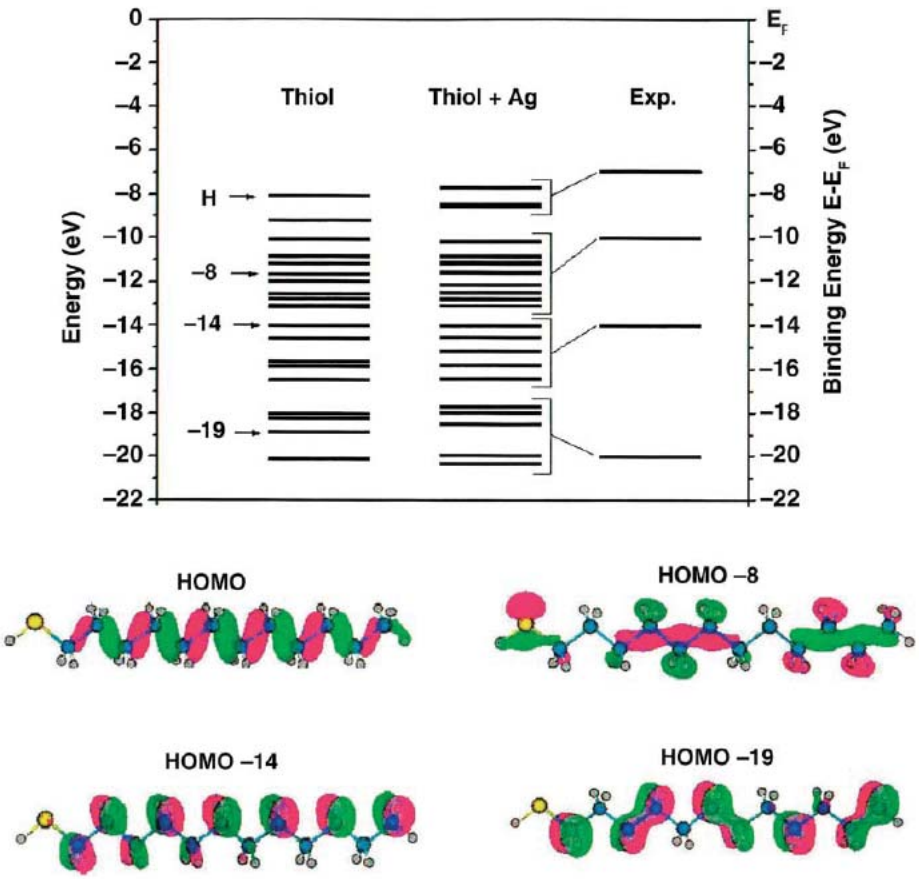

Figure 2. The calculated ground state molecular orbitals of dodecanethiol (thiol), and dodecanethiol bonded to silver (thiol + Ag), compared to the experimental photoemission features references to the Fermi level of Ag(1 1 1) without any photocharging (exp.). Selected thiol molecular orbitals are schematically shown, including the highest occupied molecular orbital (H), the highest occupied molecular orbital minus 8 (−8), the highest occupied molecular orbital minus 14 (−14), and the highest occupied molecular orbital minus 19 (−19).

to the calculated molecular orbitals obtained from density functional theory (DFT) and the perturbed molecular orbitals calculated when the hydrogen termination of the thiol, H–S–CH_2–CH_2, is replaced by silver [Ag–S–CH_2–CH_2–], for dodecanethiol. There is the typical shift of about 2.7 eV between theory and experiment [6]. The dodecanethiol photoemission peak at about 7 eV binding energy, with respect to the Fermi level and largely obscured by the Ag(1 1 1) substrate signal at low thiol coverages, is largely due to the sigma bonding along the carbon backbone chain. This feature should have a larger photoemission cross-section with the vector potential aligned parallel with the thiol chain. The photoemission peak induced by dodecanethiol adsorption at about 10 eV binding energy is an admixture of molecular orbitals that include contributions from carbon–hydrogen bonds, alkane to thiol bonding, and sigma bonding along the carbon chain. This photoemission feature will be observable in both s and p polarized light, but we anticipate that it should have stronger cross-section again with the vector potential aligned parallel with the thiol chain. Because of the multiplicity of molecular orbitals, the 7 and 10 eV binding energy features should be more difficult to resolve with increasing light polarization parallel with the alkane chain (this is observed). The photoemission feature at 14 eV binding energy is largely the result of carbon hydrogen bonds while the photoemission feature at 20 eV is a result of carbon chain π bonding molecular orbitals.

Angle-resolved photoemission measurements of the submonolayer and monolayer films provide lit-

tle indication of band structure, and the pronounced band structure, evident in angle-resolved photoemission, of the Ag(1 1 1) substrate is lost. For the thicker multilayer films adsorbed on Ag(1 1 1), we find evidence of dispersion, but this is complicated by very strong light polarization dependent photovoltaic charging. This indicates that films exhibit some two-dimensional order and again, that the thiol bonding is oriented largely normal to the surface at higher coverages. The order is limited to domains, and the thiol thin films do not form a single crystal of close packed chains, consistent with the scanning tunneling microscope (STM) results [23–27]. This indicates that the adsorption geometry of the multilayer films is drastically different from the ML films (the molecules of the monolayer films are, most likely, lying mostly parallel to the surface as expected [4, 10]). Light polarization influences on the angle-resolved photoemission spectra for the monolayer films revealed a preferred bond orientation on Ag(1 1 1) of the dodecanethiol molecular axis largely parallel with the surface at low coverage, with a more "upright" orientation indicated with the multilayer coverage, consistent with prior studies of long-chain alkane thiols on Ag(1 1 1) [13, 14]. We have not yet established that vapor deposition leads to the identical phases formed from electroless deposition under the conditions reported herein.

In the nominal metal/insulator/metal structures, weak adhesion between the alkane thiol layer(s) and the top electrode was generally found on open area samples, indicating a lack of chemical bonding to the top electrode. The resistance values of the junctions varied over several orders of magnitude without any direct correlation with junction area or molecules length. We found a lower probability of electrical shorts for heat-treated alkane thiol layer(s), which indicates that this process leads to more ordered and densely packed films. This conclusion in consistent with that found in a recent report concerning electrochemical characterization of alkane thiol layer(s) [9].

Junctions, with resistance ranging from tens of kΩ to several MΩ, were investigated. Most samples showed good temperature stability, and were capable of sustaining several temperature sweeps between room temperature and a few Kelvin. We observed a slow variation of the resistance as a function of temperature between 300 and 20–50 K. A much larger increase was observed upon lowering the temperature below 20 K (as shown in Figure 3). Such behavior is related to a large bias dependence of the differential resistance, spanning several orders of magnitude. These observations can be attributed to a Coulomb blockade caused by the Pd particles incorporated in the alkane thiol layers. If a particle is separated by a total capacitance C from the electrodes, the charging energy necessary to add one electron on the particle (i.e., $e^2/2C$) hinders the electron flow if the charging energy is significantly larger than the thermal energy [1]. From the temperature dependence of the resistance, a charging energy of several meV can be deduced, corresponding to the bias values at which the resistance of the sample diminishes significantly. This again suggests that the alkane thiol layers can form dielectric insulating layers. This systematic zero-bias anomaly is one more indication that the current flow though a limited area of the sample, not related to the total area. Studies performed on smaller junctions, with area smaller than 0.01 μm^2 [28]

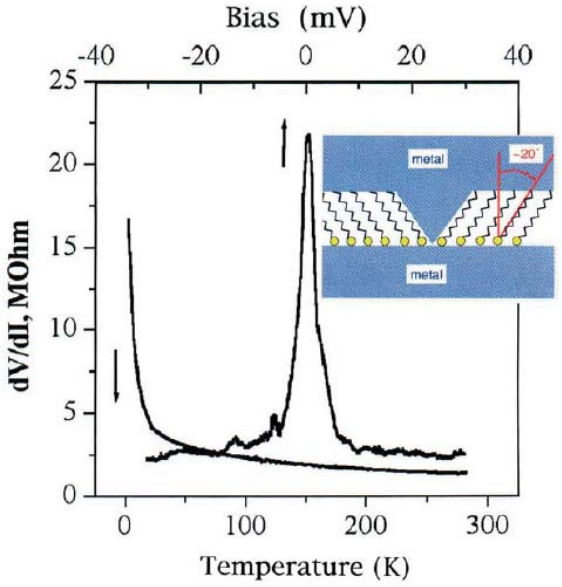

Figure 3. Zero-bias differential resistance as a function of temperature (bottom scale) and as a function of voltage bias at 1.6 K (upper scale) for Ni–ethanethiol–Ni planar junction. The limitations of the thiol structure, in high coverage monolayer films, on the formation of tunnel junction barriers.

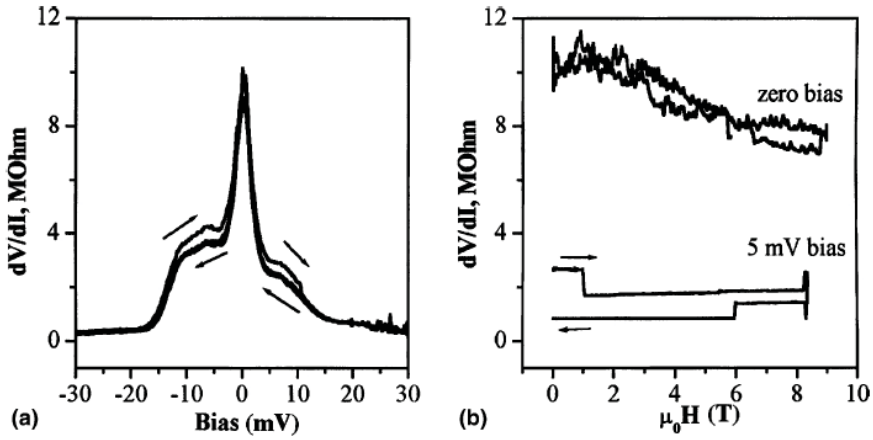

Figure 4. (a) Differential resistance of Au–dodecanothiol–Ni tunnel junction at 1.6 K as a function of applied bias. The hysteresis in the IV curves disappears after several voltage weeps, stabilizing the lower curve. (b) Magnetic field dependence for two voltage bias.

showed similar behavior. Alkane thiol "orientation" domain interfaces are likely the source of preferential current paths, as schematically indicated in Figure 3. Even if the films are a few layers thick, we observe that filamentary conduction occurs, and suspect therefore an intrinsic small orientational domain size.

A complicated dependence of the resistance on bias and applied magnetic field was observed. Asymmetrical shoulders and hysteresis on the IV curves Figure 4a were observed. Since the width of R(Bias) curve is proportional to $1/C$, where C is capacitance of particle, the appearance of shoulders could be explained by a significant parallel current channel, related to mechanical instabilities of the junction. However, significant high-field magnetoresistance, as well as steps of the magnetoresistance at bias showing hysteretic IV characteristics (Figure 4b), indicate that the magnetic state at the interfaces play a role. It is well known that a ferromagnet in close proximity to platinum or palladium will induce a magnetic moment [29–32], and thus some hysteresis might be reasonably expected from the Pd seed layer in the Au/thiol/Ni junction. Large magnetic fields are necessary to polarize significantly the palladium clusters, and it is likely that mechanical properties complicate the reproducibility and stability of the measurements. This is true of junctions as small as 10^{-2} μm^2 [28].

There is a strong indication that the thiol layers are dielectric barrier layers, nonetheless, conduction is largely limited to small regions, permitting parallel conduction pathways to form. This is consistent with the strong evidence for the insulating character of the thiol layers in photoemission, but with domain like structural character that leads to imperfections.

2. Conclusion

A variety of MIM structures were investigated, with area values varied from 10 to more than 10^2 μm^2. A systematic blocking of the current at small bias is observed, which we interpret in terms of a Coulomb blockade associated with Pd clusters. There is compelling evidence for the dielectric character of the thiol layer in photoemission of the dodecanethiol multilayers. Limits to application of thiol layers as insulating layers are clearly indicated. The absence of strong preferential chain order throughout the thiol thin film, and order that may be limited to small structural domains diminishes the efficacy of alkane thiols as a dielectric barrier in the thin film limit.

The tendency of the long-chain thiols to exhibit 13°–30° cant angles, with respect to the surface normal [2–6, 11–13, & 17], or lie flat and largely parallel with the surface [4, 10], opens wedge depressions, much like a parting of hair. Thus the top electrode will have regions of contact, or very close contact possible with the "bottom" electrode leading to small regions where the conduction path-

ways or, at the very least, parallel conduction pathways that can dominate the junction conduction.

Acknowledgements

This work was supported by the Louisiana Board of Regents Support Fund (LEQSF(2002-05)-RD-A-35 and LEQSF(2002-03)-ENH-TR-93), the National Science Foundation through the NSF "QSPINS" MRSEC (DMR 0213808) and EPSCoR program (NSF/LEQSF(2002-04)-RII-03), the Army Research Office (DAAD19-99-1-0001), the Office of Naval Research, and the Nebraska Research Initiative.

References

1. J.S. Moodera, J. Nassar and G. Mathon. *Annu. Rev. Mater. Sci.* **29** (1999), p. 381.
2. A. Ulman. *Chem. Rev.* **96** (1996), p. 1533.
3. G.E. Poirier. *Chem. Rev.* **97** (1997), p. 1117.
4. F. Schreiber. *Prog. Surf. Sci.* **65** (2000), p. 151.
5. L.H. Dubois and R.G. Nuzzo. *Annu. Rev. Phys. Chem.* **43** (1992), p. 437.
6. P.A. Dowben, J. Choi, E. Morikawa and Bo Xu. In: H.S. Nalwa, Editor, *Handbook of Thin FilmsCharacterization and Spectroscopy of Thin Films* **vol. 2**, Academic Press, New York (2002), p. 61 (Chapter 2) .
7. N. Camillone III, T.Y.B. Leung and G. Scoles. *Surf. Sci.* **373** (1997), p. 333.
8. N. Camillone III, P. Eisenberger, T.Y.B. Leung, P. Schwartz, G. Scoles, G.E. Poirier and M.J. Tarlow. *J. Chem. Phys.* **101** (1994), p. 11031.
9. N. Camillone, C.E.D. Chidsey, G.Y. Liu, T.M. Putvinski and G. Scoles. *J. Chem. Phys.* **94** (1991), p. 8493.
10. F. Schreiber, A. Eberhardt, T.Y.B. Leung, P. Schwartz, S.M. Wetterer, D.J. Lavrich, L. Berman, P. Fenter, P. Eisenberger and G. Scoles. *Phys. Rev. B* **57** (1998), p. 12476.
11. R.G. Nuzzo, E.M. Korenic and L.H. Dubois. *J. Chem. Phys.* **93** (1989), p. 767.
12. G. Hähner, M. Kinzler, C. Thümmler, Ch. Wöll and M. Grunze. *J. Vac. Sci. Technol. A* **10** (1992), p. 2758.
13. M.M. Walczak, C. Chung, S.M. Stole, C.A. Widrig and M.D. Porter. *J. Am. Chem. Soc.* **113** (1991), p. 2370.
14. Ch. Zubrägel, F. Schneider, M. Neumann, G. Hähner, Ch. Wöll and M. Grunze. *Chem. Phys. Lett.* **219** (1994), p. 127.
15. C. Boulas, J.V. Davidovits, F. Rondelez and D. Vuillaume. *Phys. Rev. Lett.* **76** (1996), p. 4797.
16. J. Collet, O. Tharaud, A. Chapoton and D. Vuillaume. *Appl. Phys. Lett.* **76** (2000), p. 1941.
17. A. Ulman, J.E. Eilers and N. Tillman. *Langmuir* **5** (1989), p. 1147.
18. M.J. Tarlov. *Langmuir* **8** (1992), p. 80.
19. P.E. Sheehan and L.J. Whitman. *Phys. Rev. Lett.* **88** (2002), p. 156104.
20. M. Schlesinger. In: M. Schlesinger and M. Paunovic, Editors, *Modern Electroplating* (fourth ed.),, Wiley, New York (2000), p. 667.
21. W. Goldie. *Plating* **51** (1964), p. 1069.
22. P.A. Dowben. *Surf. Sci. Rep.* **40** (2000), p. 151.
23. E.R. Frank, X.X. Chen and R.J. Hamers. *Surf. Sci.* **334** (1995), p. L709.
24. D. Anselmetti, A. Baratoff, H.J. Guntherodt, E. Delamarche, B. Michel, C. Gerber, H. Kang, H. Wolf and H. Ringsdorf. *Europhys. Lett.* **27** (1994), p. 365.
25. R. Berger, E. Delamarche, H.P. Lang, C. Gerber, J.K. Gimzewski, E. Meyer and H.J. Guntherodt. *Appl. Phys. A* **66** (1998), p. S55.
26. R. Berger, E. Delamarche, H.P. Lang, C. Gerber, J.K. Gimzewski, E. Meyer and H.J. Guntherodt. *Science* **276** (1997), p. 2021.
27. E. Delamarche, B. Michel, C. Gerber, D. Anselmetti, H.J. Guntherodt, H. Wolf and H. Ringsdorf. *Langmuir* **10** (1994), p. 2869.
28. Y.A Ovchenkov, C. Zhang, J. Redepenning and B. Doudin. *MRS Symp. Proc.* **745** (2003), p. 169.
29. P.F. Carcia. *J. Appl. Phys.* **63** (1988), p. 5066.
30. H.J.G. Draaisma, W.J.M. de Jonge and F.J.A. den Broeder. *J. Magn. Magn. Mater.* **66** (1987), p. 351.
31. D.M. Edwards, J. Mathon and E.P. Wohlfarth. *J. Phys. F* **3** (1973), p. 161.
32. S.D. Hwang, Y.G. Kim, C. Wu and P.A. Dowben. *Mater. Sci. Eng. B* **20** (1993), p. L1.